



HAL
open science

Detection of currents and associated electric fields in Titan's ionosphere from Cassini data

K. Agren, David J. Andrews, S. C. Buchert, A. J. Coates, S. W. H. Cowley, M. K. Dougherty, Niklas Jt Edberg, P. Garnier, G. R. Lewis, Ronan Modolo, et al.

► **To cite this version:**

K. Agren, David J. Andrews, S. C. Buchert, A. J. Coates, S. W. H. Cowley, et al.. Detection of currents and associated electric fields in Titan's ionosphere from Cassini data. *Journal of Geophysical Research Space Physics*, 2011, 116 (A4), pp.A04313. 10.1029/2010JA016100 . hal-00558003

HAL Id: hal-00558003

<https://hal.science/hal-00558003>

Submitted on 9 Jul 2020

HAL is a multi-disciplinary open access archive for the deposit and dissemination of scientific research documents, whether they are published or not. The documents may come from teaching and research institutions in France or abroad, or from public or private research centers.

L'archive ouverte pluridisciplinaire **HAL**, est destinée au dépôt et à la diffusion de documents scientifiques de niveau recherche, publiés ou non, émanant des établissements d'enseignement et de recherche français ou étrangers, des laboratoires publics ou privés.

Detection of currents and associated electric fields in Titan's ionosphere from Cassini data

K. Ågren,^{1,2} D. J. Andrews,² S. C. Buchert,¹ A. J. Coates,³ S. W. H. Cowley,² M. K. Dougherty,⁴ N. J. T. Edberg,¹ P. Garnier,⁵ G. R. Lewis,³ R. Modolo,⁶ H. Opgenoorth,¹ G. Provan,² L. Rosenqvist,⁷ D. L. Talboys,² J.-E. Wahlund,¹ and A. Wellbrock³

Received 8 September 2010; revised 15 December 2010; accepted 13 January 2011; published 19 April 2011.

[1] We present observations from three Cassini flybys of Titan using data from the radio and plasma wave science, magnetometer and plasma spectrometer instruments. We combine magnetic field and cold plasma measurements with calculated conductivities and conclude that there are currents of the order of 10 to 100 nA m⁻² flowing in the ionosphere of Titan. The currents below the exobase (~1400 km) are principally field parallel and Hall in nature, while the Pedersen current is negligible in comparison. Associated with the currents are perpendicular electric fields ranging from 0.5 to 3 μV m⁻¹.

Citation: Ågren, K., et al. (2011), Detection of currents and associated electric fields in Titan's ionosphere from Cassini data, *J. Geophys. Res.*, 116, A04313, doi:10.1029/2010JA016100.

1. Introduction

[2] Evidence of an ionosphere around Titan was first provided by occultation experiments on board Voyager 1 when it flew past the moon in 1980. An upper bound for the electron density in Titan's upper ionosphere of 2400 ± 1100 cm⁻³ at an altitude of 1180 ± 150 km was found [Bird *et al.*, 1997]. More than 20 years later, in 2004, the earliest in situ measurements of Titan's ionosphere were made during Cassini's first targeted flyby of the moon [Backes *et al.*, 2005; Wahlund *et al.*, 2005; Waite *et al.*, 2005]. The Voyager and Cassini flybys of Titan have led to extensive measurements as well as the development of numerous ionospheric models [e.g., Ip, 1990; Keller *et al.*, 1998; Galand *et al.*, 1999; Banaszkiewicz *et al.*, 2000; Cravens *et al.*, 2005; Vuitton *et al.*, 2007; Ågren *et al.*, 2007; Coates *et al.*, 2009; Cravens *et al.*, 2009; Robertson *et al.*, 2009; Wahlund *et al.*, 2009; Cui *et al.*, 2010; Edberg *et al.*, 2010]. The Cassini radio occultation experiment found a main ionospheric peak around 1200 km with a density of a few thousand cm⁻³ and another ionospheric peak with a density of 700–3000 cm⁻³ in the region of 500–600 km [Kliore *et al.*, 2008]. Furthermore, López-Moreno *et al.* [2008] used Huygens data to identify another ionospheric peak at 60–80 km altitude. Ågren *et al.* [2009] showed that

the dayside ionosphere, ranging from solar zenith angles (SZA) from 0 to 50 degrees, had a typical electron density between 2500 and 3500 cm⁻³. This corresponds to a plasma density on average four times higher than that seen on the nightside at SZA > 100 degrees, where typical densities reached 400–1000 cm⁻³. Several mechanisms contribute to the ionization of Titan's atmosphere. At altitudes around the main ionospheric peak (~900–1400 km), the main sources of ionization are considered to be photoionization by EUV from the Sun, with associated photoelectron ionization, and particle impact ionization by electrons and ions from Saturn's corotating magnetosphere. [Cravens *et al.*, 2005; Wahlund *et al.*, 2005; Galand *et al.*, 2006; Ågren *et al.*, 2009]. At lower altitudes, ionization by meteoric impacts, cosmic rays and energetic ions have been suggested to be important for the formation of the ionosphere [see, e.g., Molina-Cuberos *et al.*, 2001, and references therein]. In addition, Cui *et al.* [2009, 2010] showed that convection of plasma from the dayside might be of importance for sustaining the ionosphere on the nightside.

[3] Titan does not exhibit any large intrinsic magnetic field [Ness *et al.*, 1982; Backes *et al.*, 2005] but is normally embedded within the magnetosphere of Saturn, meaning that the magnetic field of the planet in the subcorotating flow drapes around the moon and gives rise to an induced magnetosphere. Titan orbits Saturn once every ~16 days, therefore its orbital speed of around 6 km s⁻¹ is much slower than the speed of the corotating plasma (~120 km s⁻¹). However, the configuration of this induced magnetosphere differs depending on where Titan is located with respect to Saturn's magnetosphere. It has been shown by Bertucci [2009] that the direction and magnitude of the magnetic field upstream of Titan will vary depending on whether Titan is located above or below the current sheet of Saturn. This means that the magnetic and plasma environment

¹Swedish Institute of Space Physics, Uppsala, Sweden.

²Department of Physics and Astronomy, University of Leicester, Leicester, UK.

³Mullard Space Science Laboratory, Dorking, UK.

⁴Blackett Laboratory, Imperial College, London, UK.

⁵CNRS, Toulouse, France.

⁶UVSQ/LATMOS-IPSL/CNRS-INSU, Guyancourt, France.

⁷Swedish Defence Research Agency, Stockholm, Sweden.

around Titan is very dynamic and complex and may vary substantially from flyby to flyby. Some flybys of Titan show different magnetic field configurations before and after the pass, which may imply that the magnetic background changed during the time of the flyby. For further discussion of such effects, see, e.g., *Arridge et al.* [2006, 2008], *Bertucci et al.* [2008], and *Bertucci* [2009]. We have chosen to concentrate on three flybys, namely, T18, T20, and T21, all of which show analogous flyby configurations and very similar magnetic conditions before and after the passage of the moon.

[4] *Rosenqvist et al.* [2009] performed calculations of conductivities of Titan's ionosphere, by combining electron density and magnetic field data. They identified an ionospheric dynamo region ranging from 1450 ± 95 km down to approximately 1000 km. In this region electrical currents perpendicular to the magnetic field were expected to be important, as both the Pedersen and the Hall conductivities were found to be high; $0.002\text{--}0.05$ S m⁻¹ and $0.01\text{--}0.3$ S m⁻¹, respectively.

[5] The Cassini spacecraft has been orbiting Saturn and its moons since 2004, giving a good coverage of Titan with more than 70 flybys to date. Data gathered during these passes have shown that the draped magnetic field around Titan is of the order of a few nT. Furthermore, the electron density profiles of Titan show similarities with those of Earth. Both bodies show a distinct electron peak density, although at very different altitudes, ~ 1000 km for Titan compared to ~ 300 km for Earth, due to Titan's much denser atmosphere. These facts, together with the calculated conductivities by *Rosenqvist et al.* [2009] that were mentioned above, give us reasons to believe that current systems that have been found around magnetized planets, like Earth, can be found also in the ionosphere of Titan. We expect the topologies to be quite different, as the magnetospheres of Earth and Titan are vastly different in shape and magnetic field strength. Another important difference is that the magnetic field of the currents around Titan is of the same order of magnitude as the draped magnetospheric field strength.

[6] In this paper we make a first attempt to derive ionospheric currents around Titan. In order to do so, we are forced to make assumptions on the geometry of the current systems, as our information is derived from one single spacecraft. The results will have implications for future studies of, e.g., Mars, Ganymede, and Europa, where similar current systems are probable.

[7] We use information on the short-term variation of the magnetic field around Cassini's closest approach (CA) of Titan in order to calculate magnitudes of the electric currents in the deep ionosphere of the moon. These are later combined with conductivities, to determine the current components (Hall, Pedersen and parallel) and the possible associated electric fields. We present estimates of the directions and magnitudes of the currents and the electric fields and discuss possible generation mechanisms. We note that in detailed prior models of the current system at Titan by *Ip* [1990] and *Keller et al.* [1994], the currents that switch off the field within the ionosphere are carried by horizontally drifting electrons at heights where the ions are collision dominated; that is, they are Hall currents.

[8] The paper is arranged as follows. In section 2 we introduce the instrumentation used. Sections 3–6 deal with the configuration of the flybys and present the measurements and calculations leading up to the main results of the study. In section 7 we provide a discussion of the results before ending with a summary in section 8.

2. Instrumentation

[9] This paper is based on measurements from three instruments, namely, the Cassini magnetometer (MAG), the electron spectrometer (ELS) from the Cassini plasma spectrometer (CAPS) subsystem and the radio and plasma wave science (RPWS) instrument package.

[10] MAG supplies vector components of the magnetic field with a time resolution of 1 sample s⁻¹ [*Dougherty et al.*, 2004], which are used to calculate the currents flowing in the ionosphere of Titan. CAPS/ELS is an electron spectrometer that measures electrons in the energy range 0.6 eV to 28 keV with a spatial coverage of 160 by 5 degrees [*Young et al.*, 2004].

[11] The RPWS instrument package consists of three electric field sensors, three magnetic field sensors, a spherical Langmuir probe (LP), as well as high, medium, waveform and wideband receivers for processing the data. The data presented in this study are mainly derived from the LP. However, the electric antennas are at times used to confirm the measurements, as they provide a supplementary way of obtaining the electron density from upper hybrid emissions [*Gurnett et al.*, 1982]. From the voltage-current characteristics of the LP a number of plasma parameters can be derived. These are the electron number density, n_e , the electron temperature, T_e , the ion density, n_i , the ion temperature, T_i , the ion speed, v_i , and the average ion mass, m_i . Furthermore, the LP gives information on the spacecraft potential, U_{SC} . For a more detailed discussion of the derivation of the parameters, see, e.g., *Ågren et al.* [2009] and *Wahlund et al.* [2009] while for a more extensive description of the RPWS instrument package, see *Gurnett et al.* [2004]. The electron spectra from CAPS/ELS, together with the RPWS/LP measurements, help to identify different plasma regions around Titan.

3. Flyby Configuration

[12] In this paper we focus on flybys T18, T20 and T21. Figure 1 shows the configuration of the flybys in the x-y and y-z planes in Titan centered Titan interaction coordinates (TIIS) where x is along the direction of the corotational flow, y is toward Saturn's center and z completes a right-handed orthogonal set.

[13] Another commonly used system is the kronocentric radial theta phi (KRTP) system, which is defined as follows. r is directed radially away from Saturn, θ is in the meridional direction and ϕ is in the azimuthal direction. Close to Titan, the KRTP directions are approximately the same as the TIIS, except for the sign, i.e., $\mathbf{r}_{KRTP} \sim -\mathbf{y}_{TIIS}$, $\theta_{KRTP} \sim -\theta_{TIIS}$ and $\phi_{KRTP} \sim +\phi_{TIIS}$.

[14] A third system that will be applied in this paper is a Titan-centered spherical coordinate system. It is defined as follows. r is directed radially away from Titan, θ is in the meridional direction and ϕ is in the azimuthal direction,

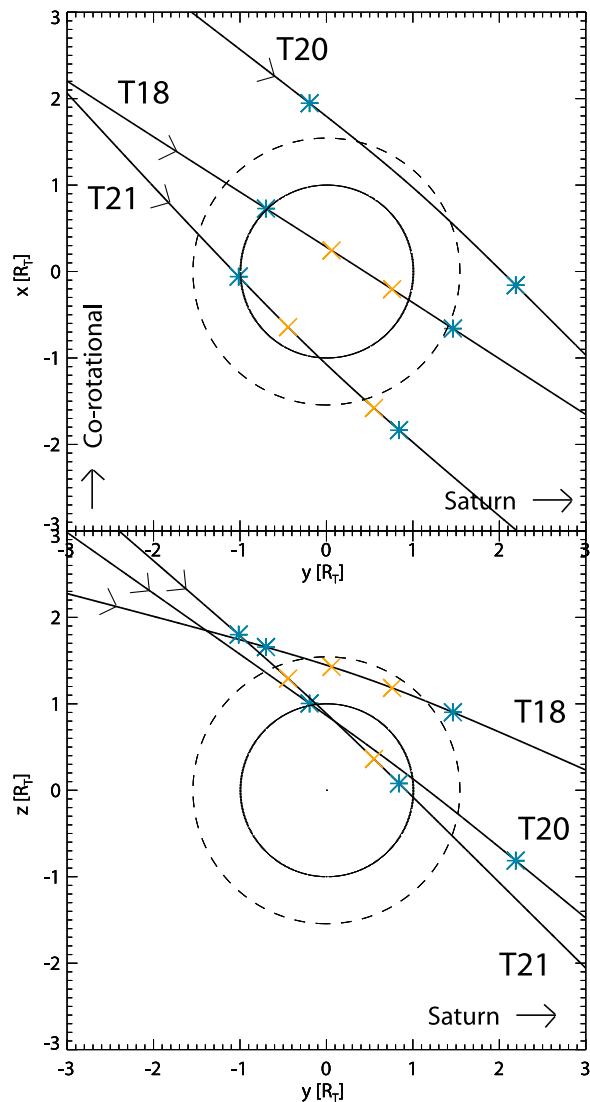


Figure 1. Configurations of the flybys T18, T20, and T21 in the (top) y - x and (bottom) y - z plane in the TIIS coordinate system. Titan is marked by the black circle, and the average position of the exobase (~ 1400 km) is indicated by the dashed circle. The straight lines give the spacecraft trajectories, with the arrows showing in which direction Cassini moves. The blue stars mark the entering of Titan's exo-ionosphere (region B), and the orange crosses indicate when Cassini goes below the ionospheric electron density peak, which is when we also see a change in the direction of the magnetic field.

with the polar axis in the $+x$ direction. As can be seen in Figure 1, T18, T20 and T21 have similar flyby configurations, with the main difference being that the T18 pass goes over the pole, the T20 pass is close to the wakeside, and the T21 pass is on the ramside of the moon. Closest approaches of the flybys are around 960 km, 1020 km and 1000 km, respectively.

[15] Choosing this set of flybys simplifies the comparison between them for two main reasons. First of all, they occur at similar Saturn local times (SLT) of 2.28 h, 2.20 h and 2.05 h, which are all located on the tailside in the post-

midnight sector of the planet. The configuration between the direction to the Sun and its photoionization, and the direction of the particle impact ionization from the subcorotating plasma flow are similar for these flybys. Second, they occurred during very similar upstream magnetic field conditions that were nearly identical before and after the Titan flyby. This is not the case for all Cassini flybys, even the ones occurring at the same SLT, due to the fact that magnetic field conditions around Titan change depending on where and at what local time in Saturn's magnetosphere the moon is located. The electron density of the corotating Kronian plasma has been shown to vary by about 2–3 orders of magnitude at a periodicity of approximately 10.7 h, which influences the magnetic conditions around Titan [Morooka *et al.*, 2009; Andrews *et al.*, 2010].

[16] During a Titan flyby, Cassini typically moves with a relative velocity of 6 km s^{-1} . Hence, the timescales of the flybys are of the order of ~ 0.5 h, which is less than the 10.7 h plasma timescale.

[17] Rymer *et al.* [2009] made a classification of the electron environment during 54 Titan passes based on ELS measurements. According to this, the three flybys chosen in our study are from very similar classes, which also facilitates the comparison. Both T20 and T21 are classified as mixed between plasma sheet and lobe-like, whereas T18 is defined as purely lobe-like. However, a recent study by Edberg *et al.* [2010] showed that the deep ionospheric plasma of Titan is similar in structure, at least in terms of the relation between the electron density and temperature, regardless of which ambient regime it is found in.

[18] Even more importantly, we have chosen these three flybys for one additional common feature. Near closest approach the magnetic field strength is declining. As predicted by the models, what we see is the exclusion of the transverse field from the lower ionosphere. In section 5 we will calculate the currents that can be associated with these changes in magnetic field direction, but first we will provide a more detailed description of the data used.

4. Titan Flyby Data

[19] Here we show the combined measurements from the ELS, LP and MAG instruments during flybys T18, T20, and T21. We start by describing the plasma data and then the magnetic field data are discussed. Figures 2a–4a show a CAPS/ELS electron spectrogram, where the color scale is on the right. Figures 2b–2d, 3b–3d, and 4b–4d show LP data, i.e., n_e , T_e , and U_{SC} , in that order. Figures 2e, 2f, 3e, 3f, 4e, and 4f show the magnetic field data in Titan-centered spherical coordinates and KRTP coordinates, respectively, with the r component shown in blue, the θ component shown in green, the ϕ component shown in orange, and the total field shown in black. By combining data from the LP and ELS instruments we can identify three regions around the moon, whose border crossings are marked by vertical lines and surrounded by shaded uncertainty regions in the plots. Region A is characterized by upstream, undisturbed magnetospheric conditions. It occurs when Titan has not yet started to influence the plasma typical of Saturn's magnetosphere and is characterized by a low ($< 1 \text{ cm}^{-3}$) electron density and high ($\sim 200 \text{ eV}$) electron temperature, which can also be verified by the electron spectra and the positive

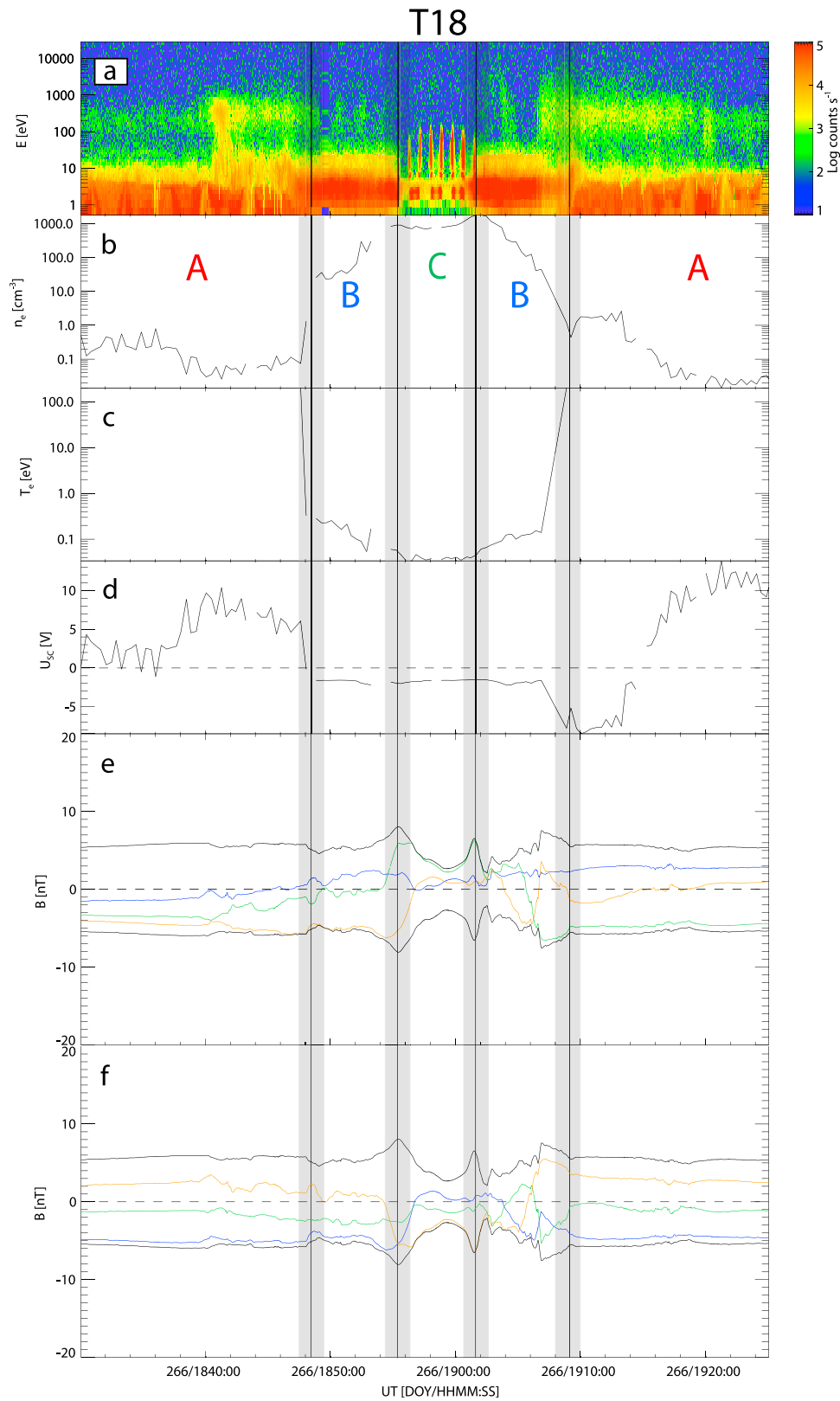


Figure 2. Time series of ELS, LP, and MAG data during the T18 flyby. (a) ELS electron spectrogram, (b) LP electron density, (c) LP electron temperature, (d) LP spacecraft potential, and MAG magnetic field components in (e) Titan-centered spherical coordinates and (f) KRTP coordinates (B_r in blue, B_θ in green, and B_ϕ in orange) and total field strength ($+B_{\text{tot}}$ and $-B_{\text{tot}}$) in black. For explanations of the vertical lines and regions A, B, and C, see the text.

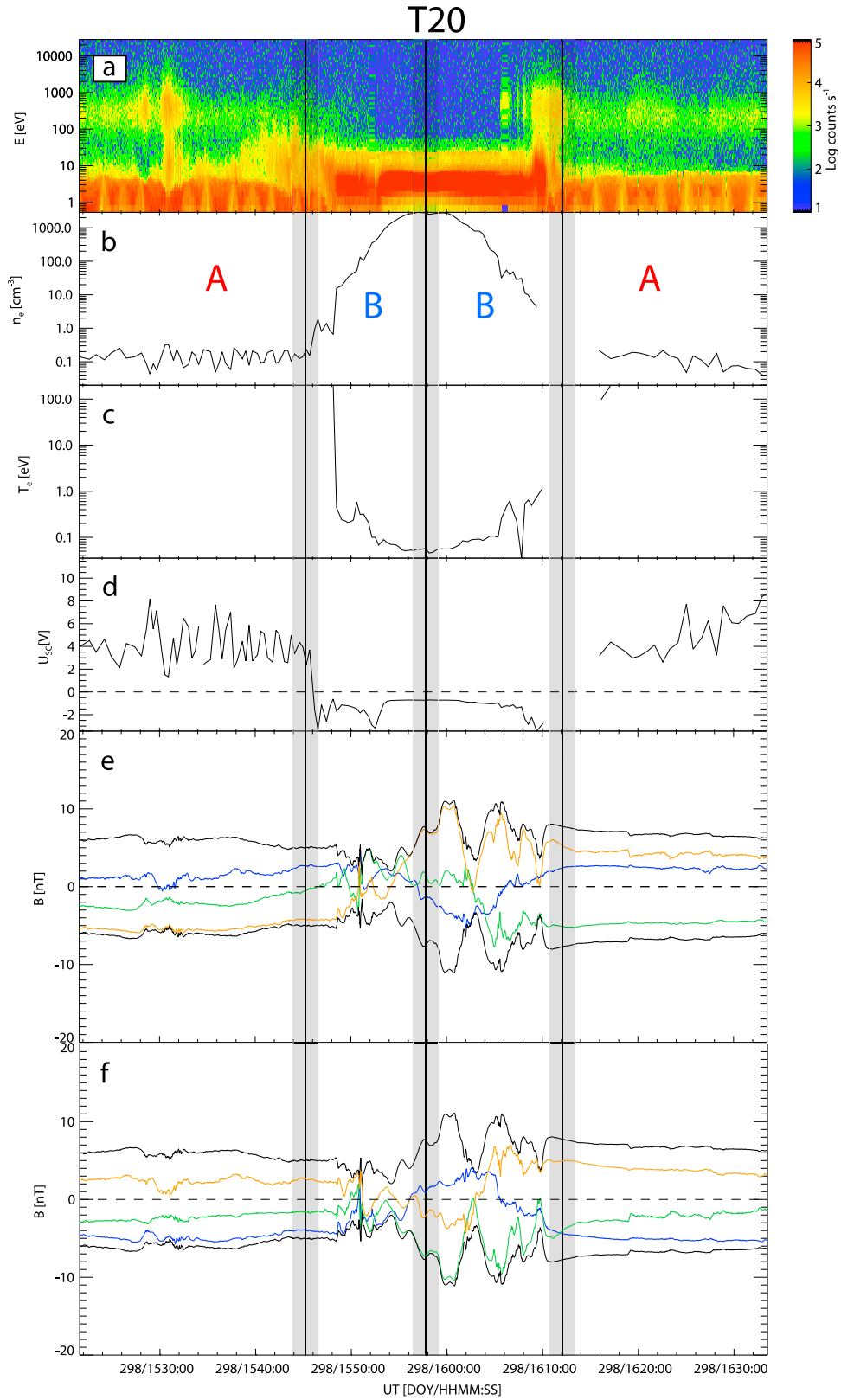


Figure 3. Same as Figure 2 except for T20. Note that region C is barely reached for this flyby, marked by the central vertical line.

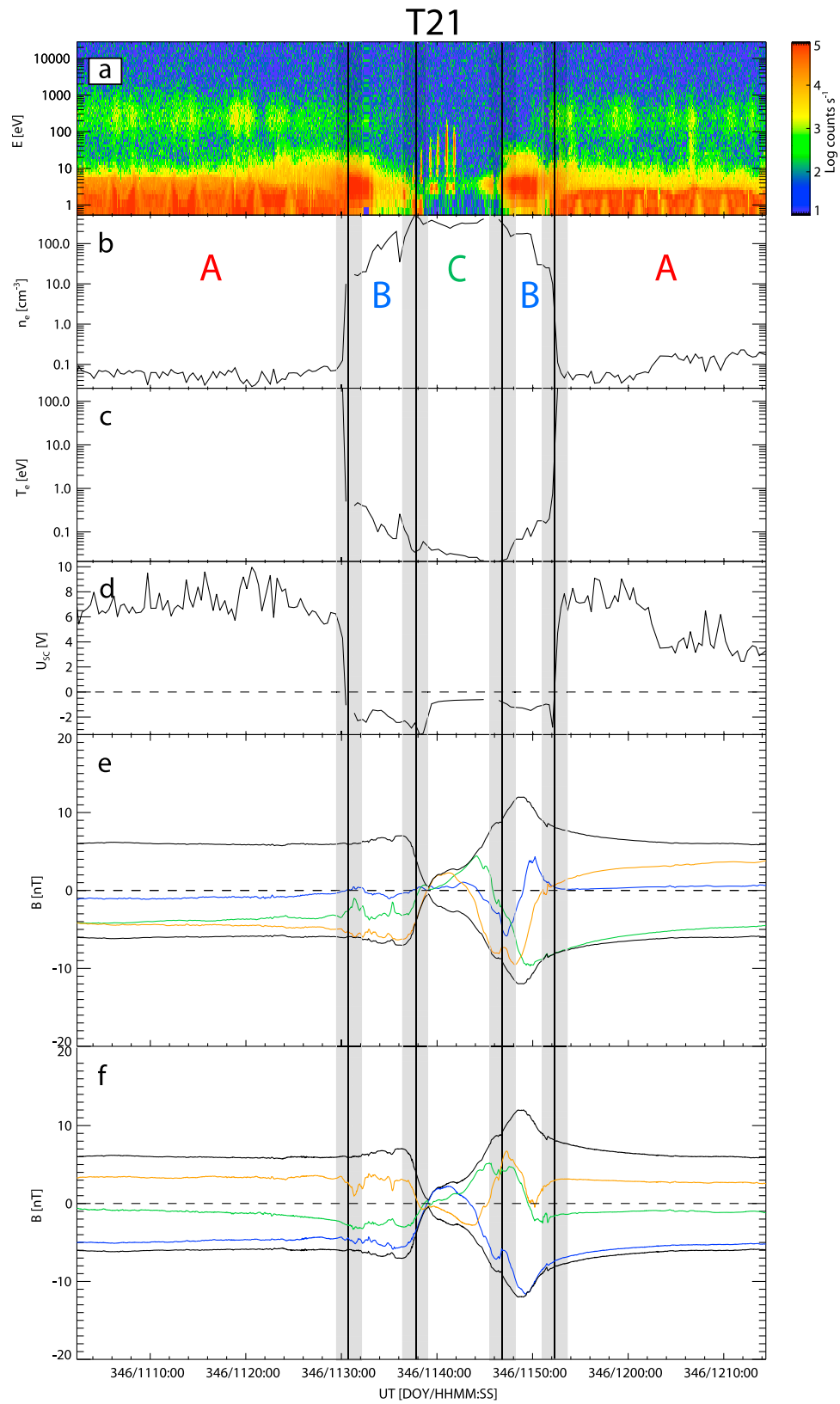


Figure 4. Same as Figure 2 except for T21.

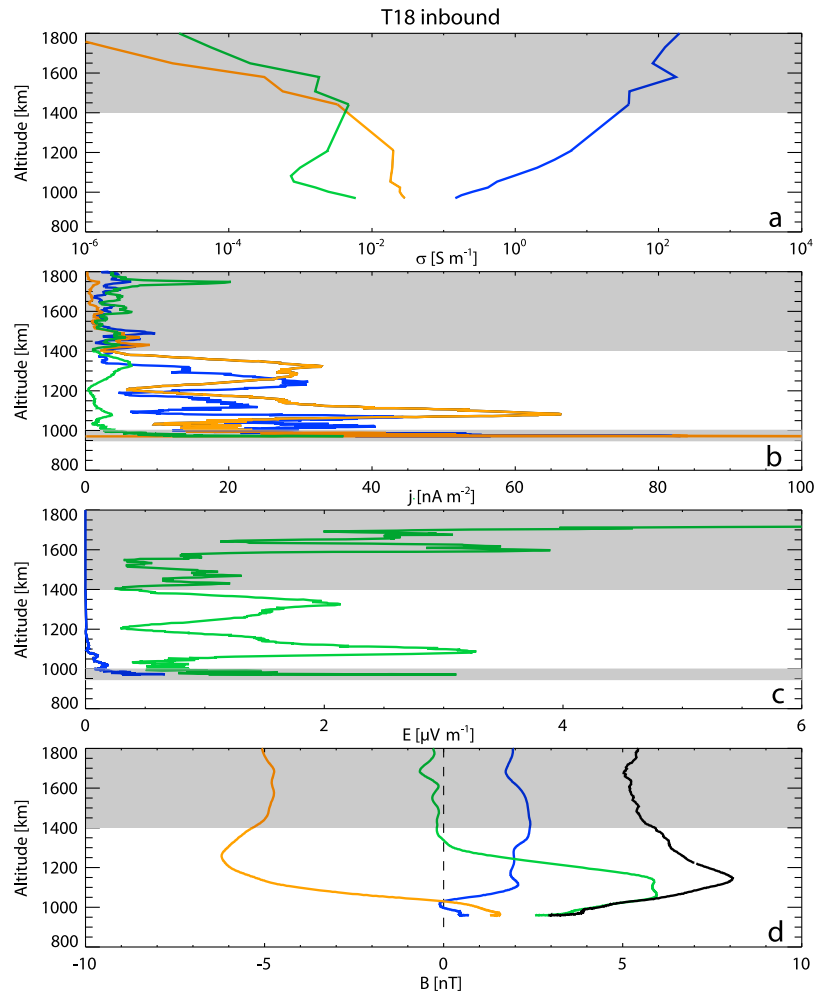


Figure 5. Data from the inbound leg of flyby T18. Altitude profiles of (a) parallel (blue), Pedersen (green), and Hall (orange) conductivities, (b) parallel (blue), Pedersen (green), and Hall (orange) currents, (c) parallel (blue) and perpendicular (green) electric fields, and (d) magnetic field components in Titan-centered spherical coordinates (B_r in blue, B_θ in green, and B_ϕ in orange) and total field strength in black.

spacecraft potential. In the next region, denoted B, the data show that the dense and cold plasma around Titan starts to dominate the measurements. In particular, the electron density shows a strong increase (about 2 orders of magnitude) at the same time as the electron temperature drops to values below 1 eV. Simultaneously, the spacecraft potential starts to change from being predominantly positive in the magnetosphere of Saturn to becoming negative in the cold plasma region around Titan. In the ELS observations (Figures 2a–4a), the region is characterized by the disappearance of spacecraft photoelectrons (with typical energies of around 1–2 eV), which is an instrumental effect due to the change in spacecraft potential, and the appearance of a new population of electrons from Titan’s ionosphere (centered at around 3 eV) and a decrease in flux of very high (>50 eV) energy electrons that characterize new plasma regimes. Region C, the ionosphere proper, is clearly seen in flybys T18 and T21, and is only just entered in T20. In this region the spacecraft goes below the ionospheric electron density peak inbound and we see a decrease in electron density with decreasing radius, followed by an increase leading up to the outbound electron density peak. The spacecraft potential (~ 1 eV),

as well as the electron temperature (~ 0.1 eV), is close to constant, and the disappearance of very low energy (<2 eV) ionospheric electrons can be seen in the ELS spectra in this region. Furthermore, the high energy precipitating electrons disappear in the observations due to collisions in the atmosphere above the spacecraft. The vertical stripes seen in the ELS spectrogram in region C are due to the detection of heavy negative ions [Coates *et al.*, 2007, 2009].

[20] Figures 2f–4f show the magnetic field data in KRTP coordinates. As discussed above, all flybys occurred during very similar ambient magnetic field conditions; that is, the magnetic field components are similar in sign and magnitude between all flybys.

[21] Changing to the Titan centered spherical coordinate system, the component of the magnetic field in the r direction (blue line) is at most times small and close to a nonzero constant, as can be seen in Figures 2e–4e. This leads to the assumption that the principal gradient of the magnetic field is in the radial distance; that is, principle field variations will be in the B_θ and B_ϕ components varying with r , indicating currents that locally mainly flow horizontally with respect to Titan’s surface. This is an essential initial

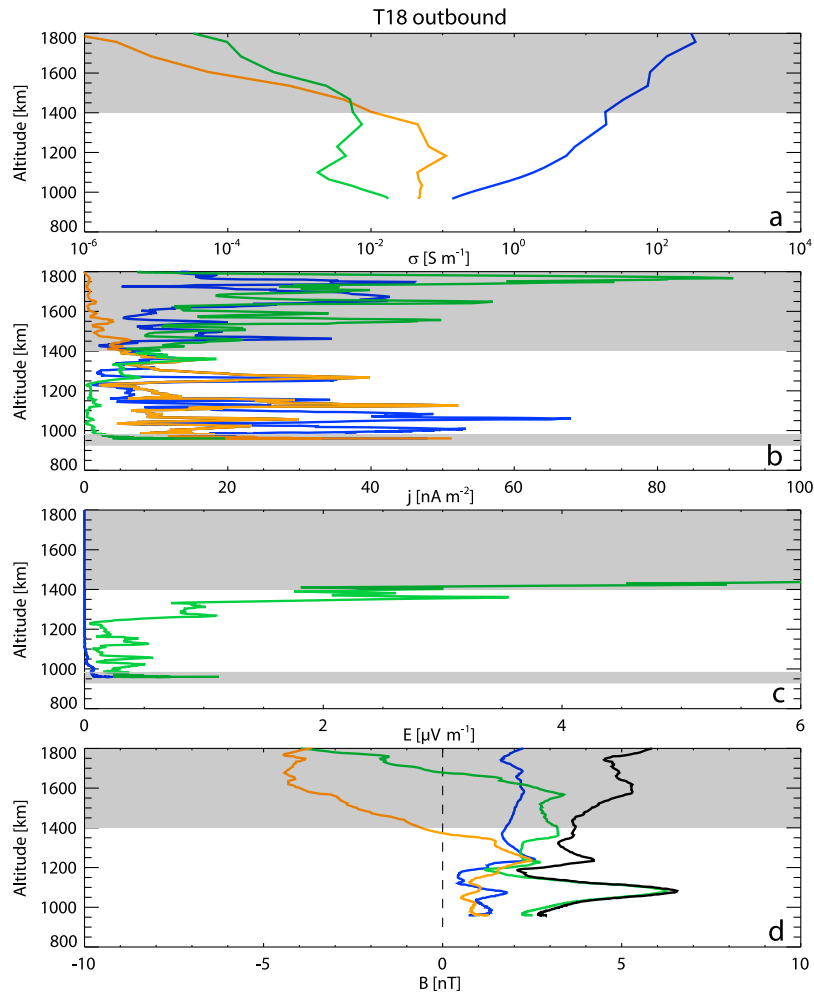


Figure 6. Same as Figure 5 except for T18 outbound.

assumption, which needs to be made as we base our observations on data from one spacecraft only. However, as can be seen in Figures 2–4, this assumption may not be valid throughout all flybys. During the inbound leg of flyby T20 and the outbound leg of flyby T21 the change of the component in the r direction is comparable to the changes in the other directions. For the remainder of this paper we will therefore concentrate on flyby T18 (both inbound and outbound), the outbound leg of flyby T20 and the inbound leg of flyby T21, where our initial assumption is most likely fulfilled. The data used correspond to approximate times of 23 September 2006 at 1851:30–1906:30 UT (T18), 25 October 2006 at 1558:30–1605:30 UT (T20), and 12 December 2006 at 1134:00–1140:30 UT (T21).

5. Calculations of the Currents

[22] Our expectation that B_θ and B_ϕ are functions of r , as was discussed above, implies ‘horizontal’ ionospheric currents in the θ and ϕ directions. By calculating the curl of the magnetic field we infer the currents in the deep ionosphere of Titan according to Ampère’s law

$$\mathbf{j} = \frac{1}{\mu_0} \nabla \times \mathbf{B}, \quad (1)$$

where $\mu_0 = 4\pi \times 10^{-7} \text{ H m}^{-1}$ is the permeability of free space. The displacement term has been neglected and a quasi-steady system assumed. Following the discussion at the end of section 4, the principal gradient of the magnetic field is expected to be in the radial direction. This means that the field mainly varies with radial distance and hence we infer currents that locally flow mainly horizontally. Thus, equation (1) can be expressed as

$$\mathbf{j} \approx \frac{1}{\mu_0} \left[\frac{1}{r} \left(-\frac{\partial}{\partial r} (rB_\phi) \right) \hat{\theta} + \frac{1}{r} \left(\frac{\partial}{\partial r} (rB_\theta) \right) \hat{\phi} \right], \quad (2)$$

where $\hat{\theta}$ and $\hat{\phi}$ are spherical unit vectors. As we know the components of the magnetic field from MAG data, we infer expressions for j_θ and j_ϕ , as well as the total current, j_{tot} . Following from this, the component of the current parallel to the magnetic field is

$$\mathbf{j}_{\parallel} = (\mathbf{j} \cdot \hat{b}) \hat{b}, \quad (3)$$

where \hat{b} is the unit vector along \mathbf{B}

$$\hat{b} = \frac{\mathbf{B}}{|\mathbf{B}|} \quad (4)$$

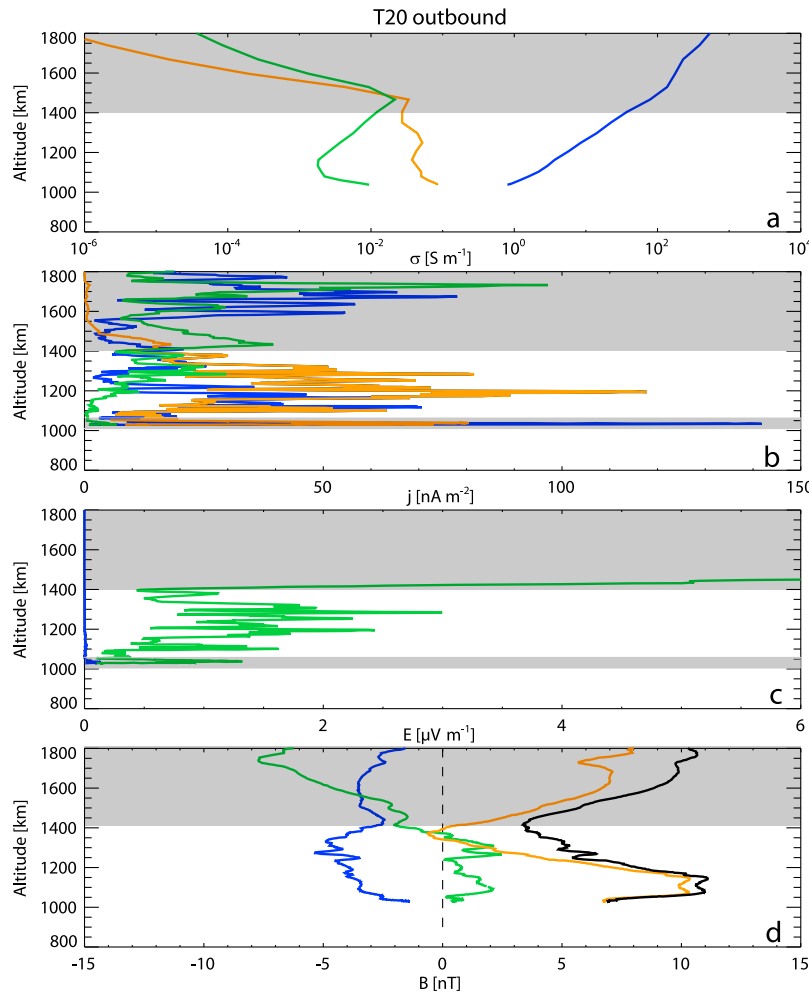


Figure 7. Same as Figure 5 except for T20 outbound.

and \mathbf{B} is the measured field, so that the perpendicular component becomes

$$\mathbf{j}_{\perp} = \mathbf{j} - \mathbf{j}_{\parallel}. \quad (5)$$

As discussed above, *Rosenqvist et al.* [2009] calculated conductivities for a total of 17 flybys, including the ones treated in this study. Figures 5a–8a show the Hall, σ_H (orange), the Pedersen, σ_P (green), and the parallel, σ_{\parallel} (blue), conductivities for T18, the outbound leg of T20 and the inbound leg of T21, respectively. These conductivities are used to estimate the Hall and Pedersen currents of the flybys. The expression for the total current is

$$\mathbf{j} = \sigma_{\parallel} \mathbf{E}_{\parallel} + \sigma_H \hat{\mathbf{b}} \times \mathbf{E}_{\perp} + \sigma_P \mathbf{E}_{\perp}, \quad (6)$$

where the first term is the parallel current, the second is the Hall current, the third is the Pedersen current and \mathbf{E}_{\parallel} and \mathbf{E}_{\perp} are the parallel and the perpendicular electric field components. E_{\perp} is the electric field in the rest frame of the neutral gas. Following from this, we derive an expression for the perpendicular current

$$\mathbf{j}_{\perp} = \sigma_H \hat{\mathbf{b}} \times \mathbf{E}_{\perp} + \sigma_P \mathbf{E}_{\perp}, \quad (7)$$

which can be solved for \mathbf{E}_{\perp}

$$\mathbf{E}_{\perp} = \frac{\sigma_H}{\sigma_P^2 + \sigma_H^2} \left[\frac{\sigma_P}{\sigma_H} \mathbf{j}_{\perp} - \hat{\mathbf{b}} \times \mathbf{j}_{\perp} \right]. \quad (8)$$

Combining equations (5), (7), and (8) we achieve expressions for the Hall and Pedersen currents. Using the parallel conductivity, we may also calculate the parallel electric field, \mathbf{E}_{\parallel} , according to

$$\mathbf{E}_{\parallel} = \frac{\mathbf{j}_{\parallel}}{\sigma_{\parallel}}. \quad (9)$$

6. Results

[23] Figures 5b–8b and 5c–8c show the magnitudes of the electric currents and the resulting electric fields plotted versus altitude as calculated from equations (2)–(9). Figures 5d–8d show the magnetic field data in Titan-centered spherical coordinates (same as in Figures 2–4) to put the data in a better relation to that from the time series plots. Below 1400 km, approximately where the exobase is

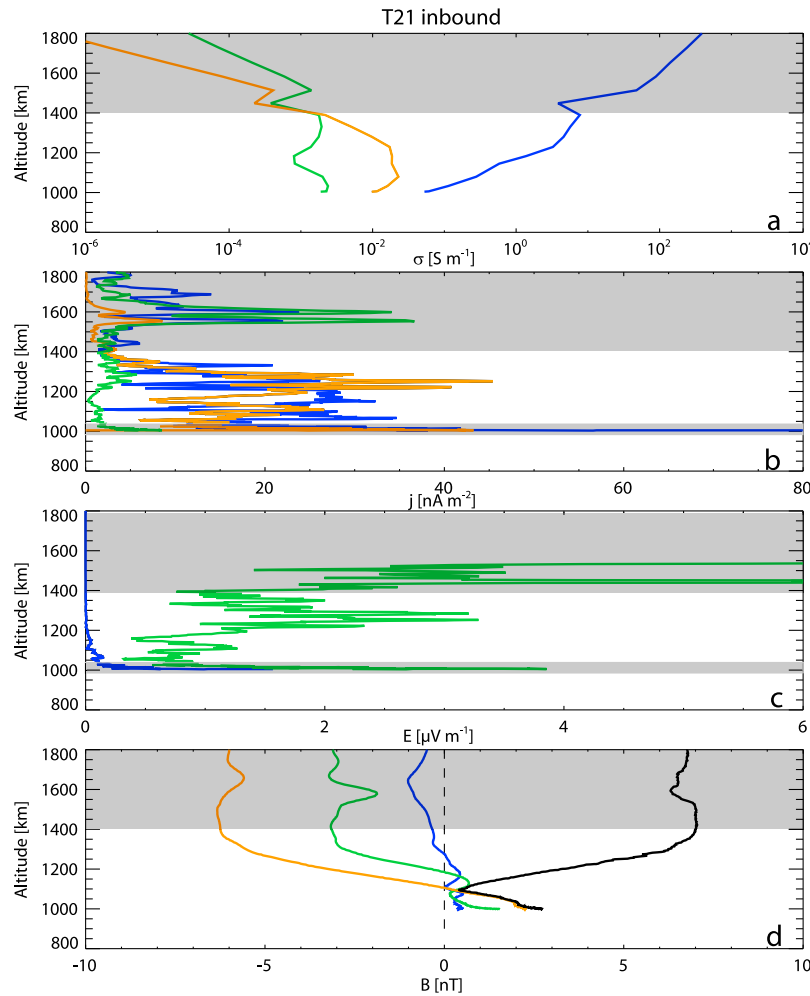


Figure 8. Same as Figure 5 except for T21 inbound.

located and collisions become important, the currents are mainly parallel and Hall in nature, meaning that they in principle are flowing parallel to the magnetic field and perpendicular to both the magnetic and the electric field, respectively. When comparing the currents from this study to the ones given by the model by *Keller et al.* [1994] there is a good agreement in both magnitude and altitude as well as the thickness of the current layer.

[24] The Pedersen current is close to zero near CA, but grows larger at altitudes above 1400 km for all investigated flybys, as the Pedersen conductivity starts to exceed the Hall conductivity. In this region the plasma becomes nonconductive across the magnetic field; that is, the parallel conductivity becomes much larger than the perpendicular one [*Rosenqvist et al.*, 2009]. This would instead indicate a possible current layer of different origin farther away from Titan. However, caution must be taken when interpreting the data at those altitudes, as transport starts to become important. Currents and electric fields above the exobase are therefore shaded in Figures 5–8.

[25] The sharp increase in currents at the lowest altitudes is a consequence of the fact that the variation in the r direction goes to zero when the spacecraft reaches CA,

leading to the breakdown of equation (2) when applied to our data. The derived current estimates in this region are therefore shaded and not reliable. However, as can be seen in Figures 5–8, this artificial feature is only detected in a very limited altitude region and does not influence our main conclusions.

[26] The resulting electric fields, in the rest frame of the neutrals (Figures 5c–8c), are seen to be predominantly perpendicular and increase with altitude above the exobase. Below the exobase, the electric fields attain values ranging from approximately 0.5 to 3 $\mu\text{V m}^{-1}$. The increase of the parallel electric field that can be seen at low altitudes is again shaded and considered to be artificial, for the same reasons that the derived currents could not be trusted around CA. Estimations of the electric field by using

$$\mathbf{E} + \mathbf{v} \times \mathbf{B} = 0 \quad (10)$$

with an ionospheric plasma speed below the exobase, v , of $\sim 1 \text{ km s}^{-1}$ given by the LP measurements and a typical value of $B = 5 \text{ nT}$ (Figures 2e–4e), predict an electric field of the order of 5 $\mu\text{V m}^{-1}$, which is in accordance with the

observations below the exobase and the fact that $\sigma_{\parallel} \gg \sigma_{\perp}$ and $E_{\parallel} \ll E_{\perp}$ at low altitudes.

7. Discussion

[27] In section 6 we derived first estimates of currents flowing in Titan's ionosphere. We investigated three flybys with similar measured magnetic field characteristics, but with the main differences that they occurred on the ramside, over the pole, and in the wake of the moon. We observed the strongest currents in the wake (up to 120 nA m^{-2}) while the ramside currents ($\sim 40 \text{ nA m}^{-2}$) and the polar currents ($\sim 60 \text{ nA m}^{-2}$) were less intense. Below the exobase, the currents are mainly Hall and parallel in nature, which seem to be displaced in phase. This is most clearly seen for flyby T18 inbound (Figure 5) and T21 (Figure 8), where the currents show opposed maxima and minima below the exobase. The magnitude of the perpendicular electric field below the exobase is $0.5\text{--}3 \mu\text{V m}^{-1}$ in all flybys.

[28] If we assume that the current is carried by electrons only, in absence of wave-particle interactions, we estimate a bulk speed of approximately 100 m s^{-1} (from $\mathbf{j} = en_e\mathbf{v}_e$) which is less than the ion acoustic speed ($\sim 600 \text{ m s}^{-1}$) confirming that an ion acoustic instability is probably not active in this region and stable current densities can exist.

[29] There are many mechanisms that could give rise to the currents observed. As Titan acts as a massive conductor in the subsonic flow of Saturn's magnetospheric plasma, the plasma flow around the moon will be deflected and produce draping of the embedded magnetic field and an exclusion of the field from inside the moon. The magnetic field is screened from the lower ionosphere, but penetrating from above due to diffusion. The currents that we observe are consistent with such diamagnetic screening currents, that could flow mainly as Hall currents in the upper ionosphere.

[30] In addition, the draping produces a tail, where a cross tail current would close partially over the outer surface. Furthermore, such a cross tail current could interact with the ionosphere via field aligned currents, to some extent similar as in the Earth's magnetotail. The plasma in the magnetosphere of Saturn at the distance of Titan typically moves with a velocity of $\sim 100 \text{ km s}^{-1}$ [Kane *et al.*, 2008; McAndrews *et al.*, 2009], and the upstream magnetic field is of the order of 5 nT , giving a maximum induced electric field strength of $500 \mu\text{V m}^{-1}$, which is more than enough to match our observations. A current system generated by associated shielding currents may set up magnetic fields that are oppositely directed to the upstream field around Titan, which is what is observed. In other words, the magnetic field on the outside, compressed and draped over the ionosphere is reduced under the ionosphere by currents in the plasma. If the ionosphere would be a perfect conductor, the magnetic field would be shielded out perfectly. However, this is not the case here as the magnetic field remains nonzero.

[31] Another mechanism that might give rise to currents is due to neutral winds in the ionosphere of Titan. Müller-Wodarg *et al.* [2008] showed that the neutral wind velocity, v_n , below the exobase reaches $\sim 150 \text{ m s}^{-1}$, which is comparable to the ion wind speed measured by Crary *et al.* [2009] of $\sim 100 \text{ m s}^{-1}$ in the same region. If we use $v_n =$

150 m s^{-1} to calculate the perpendicular electric field by using

$$\mathbf{E}_{\perp} = -\mathbf{v}_n \times \mathbf{B}, \quad (11)$$

we get an estimate of the field of $0.75 \mu\text{V m}^{-1}$, which is at the lower limit of what is observed. Hence, we do not believe this process to be the sole generation mechanism, but it might be of additional importance, preferably at low altitudes.

[32] A further possibility is to consider the currents as a result of the diffusion of fossil field lines. According to Bertucci *et al.* [2008], fossil fields oppositely directed to the ambient field may diffuse down into Titan's ionosphere. The resulting change in magnetic configuration may lead to a current, which could be measured.

[33] Examining how the magnetic field behaves long before and long after the Cassini flyby of Titan can help us constrain which generation mechanism is most probable. Looking at the flybys from this study we can conclude that the measured fields all show stable conditions. Within 3 h before and after CA we do not see any considerable changes in the magnetic field direction, which means that possible fossil fields of different orientation must be older than that. Bertucci *et al.* [2008] have estimated the convecting time of magnetic field lines in Titan's ionosphere to range between 20 min and 3 h. However, one must also keep in mind that the measurements show the environment along the Cassini orbit, which is not exactly the same as the one Titan is engulfed in.

[34] One important aspect of the current calculations is the initial assumption of how the currents are flowing. As was discussed above, our calculations only hold under the condition that the radial component of the magnetic field, B_r , is small and fairly constant. This leads to the assumption that the horizontal field components, B_{θ} and B_{ϕ} , are varying mainly with r , which through equation (2) results in currents that flow horizontally. This is why we chose to exclude the outbound leg of T20 and the inbound leg of T21, as the radial component shows a change comparable to the changes in the other directions during these legs. We believe this is a good first approximation for the selected data set. As there is a direction in which the magnetic field changes the least, we are certain that the assumption of a plane stratified horizontal current system holds. To achieve a more exact calculation one would need to do a minimum variance analysis of the magnetic field vector, but for the purposes of this paper the method we employed is valid.

8. Conclusions

[35] We have examined CAPS/ELS electron spectra, MAG magnetic field measurements and cold plasma measurements by the RPWS/LP of Titan flybys T18, T20 and T21. During these passes Cassini flew over the pole, on the wakeside and on the ramside of the moon, respectively. They all occurred at a SLT close to 2 h and showed similar upstream conditions of the magnetic field. By combining the data sets we could identify three regions around Titan. Far away from the moon the region is characterized by upstream, undisturbed magnetospheric conditions with low ($< 1 \text{ cm}^{-3}$) electron densities and high ($\sim 200 \text{ eV}$) electron

temperatures. In this region Titan has not yet started to influence the plasma typical of Saturn's magnetosphere. Closer to the moon, when the exo-ionosphere is entered, a new population of electrons from Titan's ionosphere can be identified. The electron density shows a strong increase and the electron temperature drops to values below 1 eV at the same time as the spacecraft electrons disappear due to changes in the spacecraft potential. Below the ionospheric peaks, the electron temperature does not vary much and the electron density decreases. At these altitudes the observed high-energy electrons disappear due to collisions above the spacecraft.

[36] We have shown that, indeed, during at least some instances, there are strong horizontal currents of the order of 10–100 nA m⁻² flowing in the ionosphere of Titan. This is to the best of our knowledge the first observations of ionospheric currents at the moon. Below approximately 1400 km the currents are principally parallel and Hall, i.e., flowing parallel to the magnetic field and perpendicular to both the magnetic field and the electric field, respectively. At higher altitudes the Pedersen current seemingly becomes more prominent, which may instead be due to current layers produced by the interaction boundaries between Saturn's magnetosphere and Titan's ionospheric plasma. However, our data is yet insufficient to make such local discriminations. More detailed, and hopefully some day even multi-spacecraft data, will be required to address these and further questions in the future. Associated with the ionospheric currents are electric fields of the order of 0.5–3 μV m⁻¹. In the region below 1400 km the electric fields are predominantly perpendicular to the magnetic field.

[37] **Acknowledgments.** K.Å. conducted a major part of this work at the University of Leicester while working on a Marie Curie Host Fellowship for Early Stage Researchers. The Swedish National Space Board (SNSB) supports the RPWS/LP instrument on board Cassini. D.J.A. was supported by a STFC quota studentship, and D.L.T. was supported by STFC grant SG 371 PP/D002117/1. K.Å. also wants to acknowledge numerous interesting and fruitful discussions with fil. lic. Erik Nordblad at the Swedish Institute of Space Physics.

[38] Robert Lysak thanks the reviewers for their assistance in evaluating this paper

References

- Ågren, K., et al. (2007), On magnetospheric electron impact ionisation and dynamics in Titan's ram-side and polar ionosphere—A Cassini case study, *Ann. Geophys.*, *25*, 2359–2369.
- Ågren, K., J. Wahlund, P. Garnier, R. Modolo, J. Cui, M. Galand, and I. Müller-Wodarg (2009), On the ionospheric structure of Titan, *Planet. Space Sci.*, *57*, 1821–1827, doi:10.1016/j.pss.2009.04.012.
- Andrews, D. J., S. W. H. Cowley, M. K. Dougherty, and G. Provan (2010), Magnetic field oscillations near the planetary period in Saturn's equatorial magnetosphere: Variation of amplitude and phase with radial distance and local time, *J. Geophys. Res.*, *115*, A04212, doi:10.1029/2009JA014729.
- Arridge, C. S., N. Achilleos, M. K. Dougherty, K. K. Khurana, and C. T. Russell (2006), Modeling the size and shape of Saturn's magnetopause with variable dynamic pressure, *J. Geophys. Res.*, *111*, A11227, doi:10.1029/2005JA011574.
- Arridge, C. S., K. K. Khurana, C. T. Russell, D. J. Southwood, N. Achilleos, M. K. Dougherty, A. J. Coates, and H. K. Leinweber (2008), Warping of Saturn's magnetospheric and magnetotail current sheets, *J. Geophys. Res.*, *113*, A08217, doi:10.1029/2007JA012963.
- Backes, H., et al. (2005), Titan's magnetic field signature during the first Cassini encounter, *Science*, *308*, 992–995, doi:10.1126/science.1109763.
- Banaszkiewicz, M., L. M. Lara, R. Rodrigo, J. J. López-Moreno, and G. J. Molina-Cuberos (2000), A coupled model of Titan's atmosphere and ionosphere, *Icarus*, *147*, 386–404, doi:10.1006/icar.2000.6448.
- Bertucci, C. L. (2009), Characteristics and variability of Titan's magnetic environment, *Philos. Trans. R. Soc. A*, *367*, 789–798, doi:10.1098/rsta.2008.0250.
- Bertucci, C., et al. (2008), The magnetic memory of Titan's ionized atmosphere, *Science*, *321*, 1475–1478, doi:10.1126/science.1159780.
- Bird, M. K., R. Dutta-Roy, S. W. Asmar, and T. A. Rebold (1997), Detection of Titan's ionosphere from Voyager 1 radio occultation observations, *Icarus*, *130*, 426–436, doi:10.1006/icar.1997.5831.
- Coates, A. J., F. J. Crary, G. R. Lewis, D. T. Young, J. H. Waite, and E. C. Sittler (2007), Discovery of heavy negative ions in Titan's ionosphere, *Geophys. Res. Lett.*, *34*, L22103, doi:10.1029/2007GL030978.
- Coates, A. J., A. Wellbrock, G. R. Lewis, G. H. Jones, D. T. Young, F. J. Crary, and J. H. Waite (2009), Heavy negative ions in Titan's ionosphere: Altitude and latitude dependence, *Planet. Space Sci.*, *57*, 1866–1871, doi:10.1016/j.pss.2009.05.009.
- Crary, F. J., B. A. Magee, K. Mandt, J. H. Waite, J. Westlake, and D. T. Young (2009), Heavy ions, temperatures and winds in Titan's ionosphere: Combined Cassini CAPS and INMS observations, *Planet. Space Sci.*, *57*, 1847–1856, doi:10.1016/j.pss.2009.09.006.
- Cravens, T. E., et al. (2005), Titan's ionosphere: Model comparisons with Cassini Ta data, *Geophys. Res. Lett.*, *32*, L12108, doi:10.1029/2005GL023249.
- Cravens, T. E., et al. (2009), Model-data comparisons for Titan's nightside ionosphere, *Icarus*, *199*, 174–188, doi:10.1016/j.icarus.2008.09.005.
- Cui, J., et al. (2009), Diurnal variations of Titan's ionosphere, *J. Geophys. Res.*, *114*(A13), A06310, doi:10.1029/2009JA014228.
- Cui, J., M. Galand, R. V. Yelle, J. Wahlund, K. Ågren, J. H. Waite, and M. K. Dougherty (2010), Ion transport in Titan's upper atmosphere, *J. Geophys. Res.*, *115*, A06314, doi:10.1029/2009JA014563.
- Dougherty, M. K., et al. (2004), The Cassini magnetic field investigation, *Space Sci. Rev.*, *114*, 331–383, doi:10.1007/s11214-004-1432-2.
- Edberg, N. J. T., J.-E. Wahlund, K. Ågren, M. W. Morooka, R. Modolo, C. Bertucci, and M. K. Dougherty (2010), Electron density and temperature measurements in the cold plasma environment of Titan: Implication for atmospheric escape, *Geophys. Res. Lett.*, *37*, L20105, doi:10.1029/2010GL044544.
- Galand, M., J. Liliensten, D. Toublanc, and S. Maurice (1999), The ionosphere of Titan: Ideal diurnal and nocturnal cases, *Icarus*, *140*, 92–105, doi:10.1006/icar.1999.6113.
- Galand, M., R. V. Yelle, A. J. Coates, H. Backes, and J.-E. Wahlund (2006), Electron temperature of Titan's sunlit ionosphere, *Geophys. Res. Lett.*, *33*, L21101, doi:10.1029/2006GL027488.
- Gurnett, D. A., F. L. Scarf, and W. S. Kurth (1982), The structure of Titan's wake from plasma wave observations, *J. Geophys. Res.*, *87*, 1395–1403.
- Gurnett, D. A., et al. (2004), The Cassini radio and plasma wave investigation, *Space Sci. Rev.*, *114*, 395–463, doi:10.1007/s11214-004-1434-0.
- Ip, W. (1990), Titan's upper ionosphere, *Astrophys. J.*, *362*, 354–363, doi:10.1086/169271.
- Kane, M., D. G. Mitchell, J. F. Carbary, S. M. Krimigis, and F. J. Crary (2008), Plasma convection in Saturn's outer magnetosphere determined from ions detected by the Cassini INCA experiment, *Geophys. Res. Lett.*, *35*, L04102, doi:10.1029/2007GL032342.
- Keller, C. N., T. E. Cravens, and L. Gan (1994), One-dimensional multi-species magnetohydrodynamic models of the ramside ionosphere of Titan, *J. Geophys. Res.*, *99*, 6511–6525, doi:10.1029/93JA02680.
- Keller, C. N., V. G. Anicich, and T. E. Cravens (1998), Model of Titan's ionosphere with detailed hydrocarbon ion chemistry, *Planet. Space Sci.*, *46*, 1157–1174.
- Kliore, A. J., et al. (2008), First results from the Cassini radio occultations of the Titan ionosphere, *J. Geophys. Res.*, *113*, A09317, doi:10.1029/2007JA012965.
- López-Moreno, J. J., et al. (2008), Structure of Titan's low altitude ionized layer from the Relaxation Probe onboard Huygens, *Geophys. Res. Lett.*, *35*, L22104, doi:10.1029/2008GL035338.
- McAndrews, H. J., et al. (2009), Plasma in Saturn's nightside magnetosphere and the implications for global circulation, *Planet. Space Sci.*, *57*, 1714–1722, doi:10.1016/j.pss.2009.03.003.
- Molina-Cuberos, G. J., H. Lammer, W. Stumptner, K. Schwingenschuh, H. O. Rucker, J. J. Lopez-Moreno, R. Rodrigo, and T. Tokano (2001), Ionospheric layer induced by meteoric ionization in Titan's atmosphere, *Planet. Space Sci.*, *49*, 143–153.
- Morooka, M. W., et al. (2009), The electron density of Saturn's magnetosphere, *Ann. Geophys.*, *27*, 2971–2991.
- Müller-Wodarg, I. C. F., R. V. Yelle, J. Cui, and J. H. Waite (2008), Horizontal structures and dynamics of Titan's thermosphere, *J. Geophys. Res.*, *113*, E10005, doi:10.1029/2007JE003033.
- Ness, N. F., M. H. Acuna, and K. W. Behannon (1982), The induced magnetosphere of Titan, *J. Geophys. Res.*, *87*, 1369–1381.

- Robertson, I. P., et al. (2009), Structure of Titan's ionosphere: Model comparisons with Cassini data, *Planet. Space Sci.*, *57*, 1834–1846, doi:10.1016/j.pss.2009.07.011.
- Rosenqvist, L., J. Wahlund, K. Ågren, R. Modolo, H. J. Opgenoorth, D. Strobel, I. Müller-Wodarg, P. Garnier, and C. Bertucci (2009), Titan ionospheric conductivities from Cassini measurements, *Planet. Space Sci.*, *57*, 1828–1833, doi:10.1016/j.pss.2009.01.007.
- Rymer, A. M., H. T. Smith, A. Wellbrock, A. J. Coates, and D. T. Young (2009), Discrete classification and electron energy spectra of Titan's varied magnetospheric environment, *Geophys. Res. Lett.*, *36*, L15109, doi:10.1029/2009GL039427.
- Vuitton, V., R. V. Yelle, and M. J. McEwan (2007), Ion chemistry and N-containing molecules in Titan's upper atmosphere, *Icarus*, *191*, 722–742, doi:10.1016/j.icarus.2007.06.023.
- Wahlund, J.-E., et al. (2005), Cassini measurements of cold plasma in the ionosphere of Titan, *Science*, *308*, 986–989, doi:10.1126/science.1109807.
- Wahlund, J.-E., et al. (2009), On the amount of heavy molecular ions in Titan's ionosphere, *Planet. Space Sci.*, *57*, 1857–1865, doi:10.1016/j.pss.2009.07.014.
- Waite, J. H., et al. (2005), Ion neutral mass spectrometer results from the first flyby of Titan, *Science*, *308*, 982–986, doi:10.1126/science.1110652.
- Young, D. T., et al. (2004), Cassini plasma spectrometer investigation, *Space Sci. Rev.*, *114*, 1–112, doi:10.1007/s11214-004-1406-4.
-
- K. Ågren, S. C. Buchert, N. J. T. Edberg, H. Opgenoorth, and J.-E. Wahlund, Swedish Institute of Space Physics, Box 537, SE-751 21, Uppsala, Sweden. (agren@irfu.se)
- D. J. Andrews, S. W. H. Cowley, G. Provan, and D. L. Talboys, Department of Physics and Astronomy, University of Leicester, University Road, Leicester LE1 7RH, UK.
- A. J. Coates, G. R. Lewis, and A. Wellbrock, Mullard Space Science Laboratory, Dorking RH5 6NT, UK.
- M. K. Dougherty, Blackett Laboratory, Imperial College London, Prince Consort Road, London SW7 2BW, UK.
- P. Garnier, CNRS, 14 Avenue Edouard Belin, F-31400 Toulouse, France.
- R. Modolo, LATMOS, Quartier des Garennes, 11bd d'Alembert, F-78280 Guyancourt, France.
- L. Rosenqvist, Swedish Defence Research Agency, SE-164 90 Stockholm, Sweden.